RESEARCH ARTICLE | DECEMBER 04 2024

Black-box optimization technique for investigation of surface phase diagram

Makoto Urushihara ✉; Kenji Yamaguchi ; Ryo Tamura ✉

AIP Advances 14, 125008 (2024)
https://doi.org/10.1063/5.0229856

Black-box optimization technique for investigation of surface phase diagram

Cite as: AIP Advances 14, 125008 (2024); doi: 10.1063/5.0229856
Submitted: 19 July 2024 • Accepted: 17 November 2024 •
Published Online: 4 December 2024

Makoto Urushihara,[1,a)] Kenji Yamaguchi,[1] and Ryo Tamura[2,3,a)]

AFFILIATIONS

[1] Innovation Center, Mitsubishi Materials Corporation, 1002-14 Mukohyama, Naka, Ibaraki 311-0102, Japan
[2] Center for Basic Research on Materials, National Institute for Materials Science, 1-1 Namiki, Tsukuba, Ibaraki 305-0044, Japan
[3] Graduate School of Frontier Sciences, The University of Tokyo, 5-1-5 Kashiwa-no-ha, Kashiwa, Chiba 277-8561, Japan

[a)] **Authors to whom correspondence should be addressed:** urushi@mmc.co.jp and tamura.ryo@nims.go.jp

ABSTRACT

Surface phase diagrams are useful in material design for understanding catalytic reactions and deposition processes and are usually obtained by numerical calculations. However, a large number of calculations are required, and a strategy to reduce the computation time is necessary. In this study, we proposed a black-box optimization strategy to investigate the surface phase diagram with the smallest possible number of calculations. Our method was tested to examine the phase diagram in which two types of adsorbates, i.e., oxygen and carbon monoxide, were adsorbed onto a palladium surface. In comparison with a random calculation without using machine learning, we confirmed that the proposed method obtained a surface phase diagram with a small number of calculations. In conclusion, our strategy is a general-purpose method that can contribute to the rapid study of various types of surface phase diagrams.

I. INTRODUCTION

A surface phase diagram describes the state of adsorption between a gas or liquid molecules on a solid surface,[1,2] i.e., depending on the thermodynamic parameters such as temperature, pressure, and chemical potential, the stable adsorption structures are summarized. Surface phase diagrams are widely used in material design to understand catalytic reactions and deposition processes.[3–7] However, the microscopic atomistic structures on surfaces with adsorbates are difficult to detect experimentally using current measurement technologies and, therefore, the construction of surface phase diagrams relies on atomistic simulations. Even with simulations, constructing a surface phase diagram is a time-consuming task that requires many calculations while changing the thermodynamic parameters.

The general procedure for constructing a surface phase diagram based on the chemical potentials of each adsorbate using atomistic simulations is described as follows.[8,9] First, we search for stable adsorption structures based on density functional theory (DFT) calculations when the surface coverage of adsorbates is varied and calculate the adsorption energy for each stable structure. Second, we identify the stable adsorption structure with the lowest adsorption energy depending on the chemical potential and obtain a surface phase diagram. The first step of the procedure requires a large number of calculations because there are a large number of combinations according to the different numbers of adsorbates to be adsorbed on the surface. In addition, if the number of molecules is fixed, a stable adsorption structure is difficult to find, and long-term simulations based on DFT calculations are needed.

Here, we propose a black-box optimization (BBO) method to reduce the number of calculations required to construct surface phase diagrams. BBO is frequently used in materials science to optimize materials with desired physical properties through a small number of experiments or calculations.[10] Various methods have been developed to meet research needs; some methods have also been proposed for constructing phase diagrams.[11–16] However, these methods cannot be directly applied to surface phase diagrams, and the development of an appropriate method is required. The BBO method for surface diagrams has been considered an efficient construction method for Pourbaix diagrams with one-dimensional parameters, i.e., applied potential.[17] Still, the extension to surface diagrams with multiple parameters beyond the two-dimensional

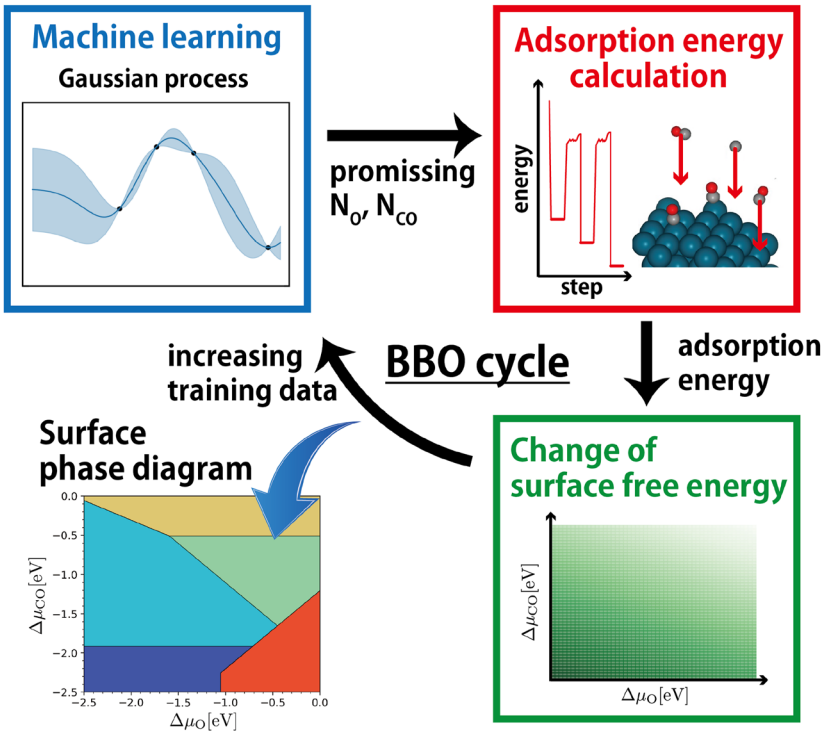

FIG. 1. Flow chart of the proposed black-box optimization (BBO) method to construct a surface phase diagram.

space has not been considered. In this study, we developed a BBO method that could treat multiple parameters such as the chemical potentials of adsorbates. The flow chart of the proposed BBO method is illustrated in Fig. 1. The parameter targeted for optimization is the number of adsorbates on the surface, which is defined as $\{N_k\}_{k=1,\ldots,K}$, where K types of adsorbates are adsorbed. The acquisition function is defined by the change of surface free energy with respect to adsorption, which is expressed as $\Delta(\{N_k\}_{k=1,\ldots,K})$. The stable adsorption structure with a small $\Delta(\{N_k\}_{k=1,\ldots,K})$ value appears in a large area of the surface phase diagram. In the BBO method, iterative calculations are performed to acquire better conditions for the numbers of molecules with small $\Delta(\{N_k\}_{k=1,\ldots,K})$. The Gaussian process regression (GPR) model is trained from the initial data under some conditions with stable adsorption energies. Based on the predicted results of the GPR model, one condition for the numbers of adsorbates is selected. Under the selected condition, a stable adsorption structure is determined using atomistic simulations. Because the number of training data points increased by one, the next condition is selected using the retrained GPR model. Therefore, in every iteration, an atomistic simulation is required to determine a stable adsorption structure when the number of molecules is fixed. The motivation for the proposed BBO is to reduce the number of investigated conditions to obtain details of the surface phase diagram.

II. METHOD

We describe the details of the proposed BBO method. First, as initial data, we search for adsorption structures that are stable for some conditions of $\{N_k\}_{k=1,\ldots,K}$. In this study, the constrained minima hopping method[18] implemented in the atomistic simulation environment (ASE) package[19] is used. Normally, DFT calculations are used to evaluate the adsorption energy. However, to reduce the computation time, the adsorption energies were evaluated using the neural network potentials by Matlantis.[20,21] The details of the calculation method are described in Supplemental Note A. The adsorption energy of the explored stable adsorption structure obtained by combining the minima hopping method and Matlantis is expressed as $E_{\mathrm{abs}}(N_1, N_2, \ldots, N_K)$, which is a function of the numbers of adsorbates. Instead of the constrained minima hopping method, other optimization techniques such as the annealing approach[22] and BBO methods[23,24] can be used to search for stable adsorption structures.[25,26] Using the obtained $E_{\mathrm{abs}}(N_1, N_2, \ldots, N_K)$, the free energy changes due to adsorption depending on the chemical potentials of each type of molecule $\{\Delta\mu_k\}_{k=1,\ldots,K}$ are defined approximately as follows:

$$\Delta G(N_1, N_2, \ldots, N_K | \Delta\mu_1, \Delta\mu_2, \ldots, \Delta\mu_K) \sim \frac{1}{A(N_1, N_2, \ldots, N_K)} \times \left(E_{\mathrm{abs}}(N_1, N_2, \ldots, N_K) - \sum_{k=1}^{K} N_k \Delta\mu_k \right), \quad (1)$$

where $A(N_1, N_2, \ldots, N_K)$ is the surface area where the adsorbates are adsorbed.

Next, we construct a machine learning model to predict the adsorption energy from arbitrary $\{N_k\}_{k=1,\ldots,K}$. If there are M conditions for the number of adsorbed adsorbates where the adsorption energy has already been calculated, these data are used as training data for the GPR model, which is trained using Scikit-learn.[27] The

GPR model can compute not only the mean $\mu(N_1, N_2, \ldots, N_K)$ but also the variance $\sigma(N_1, N_2, \ldots, N_K)$ of prediction. Considering the variance, which is the uncertainty of the prediction, we define the predicted adsorption energy as

$$E^*_{\mathrm{abs}}(N_1, N_2, \ldots, N_K) = \mu(N_1, N_2, \ldots, N_K) - \beta\sigma(N_1, N_2, \ldots, N_K). \tag{2}$$

If the adsorption energy is low, the corresponding adsorption structure has a greater impact on the surface phase diagram. Therefore, we define $E^*_{\mathrm{abs}}(N_1, N_2, \ldots, N_K)$ as the lower bound, including the prediction uncertainty, based on the concept of the lower confidence bound (LCB) strategy.[28] Here, β is a hyperparameter, and the uncertainty of prediction becomes important in $E^*_{\mathrm{abs}}(N_1, N_2, \ldots, N_K)$ with a larger β. Therefore, the predicted free energy changes due to adsorption depending on $\{N_k\}_{k=1,\ldots,K}$ can be approximated as

$$\Delta G^*(N_1, N_2, \ldots, N_K | \Delta\mu_1, \Delta\mu_2, \ldots, \Delta\mu_K) \sim \frac{1}{A(N_1, N_2, \ldots, N_K)} \times \left(E^*_{\mathrm{abs}}(N_1, N_2, \ldots, N_K) - \sum_{k=1}^{K} N_k \Delta\mu_k \right). \tag{3}$$

The predicted surface phase diagram is obtained using the prediction model. In the predicted case, the conditions for the numbers of adsorbed molecules with small free energies over a wide region are dominant. Based on this fact, we define an acquisition function to select the condition such that the corresponding stable structure appears in the surface phase diagram over a wide region.

To define the acquisition function, we consider a discretized surface phase diagram, i.e., the chemical potentials are discretized. When the sum of the free energies at all discretized points is small, the corresponding condition is expected to appear over a large area of the surface phase diagram. Therefore, the acquisition function based on the predicted free-energy changes is defined as

$$\Delta(\{N_k\}_{k=1,\ldots,K}) = \sum_{\Delta\mu_1} \sum_{\Delta\mu_2} \cdots \sum_{\Delta\mu_K} \frac{1}{A(N_1, N_2, \ldots, N_K)} \times \left(E^*_{\mathrm{abs}}(N_1, N_2, \ldots, N_K) - \sum_{k=1}^{K} N_k \Delta\mu_k \right), \tag{4}$$

where the sums are performed on the discretized chemical potential values. For all candidate conditions with different numbers of adsorbates to be adsorbed, $\Delta(\{N_k\}_{k=1,\ldots,K})$ is evaluated, and one condition with minimum value is selected. For the selected condition, the adsorption energy is calculated using the constrained minima hopping method and Matlantis. Then, the amount of data is increased to prepare $M+1$ training data. The GPR model is retrained, and the next condition is selected for iterative calculations.

III. RESULTS

To clarify the performance of the proposed BBO method in constructing a surface phase diagram, we addressed the problem in which two types of adsorbates, i.e., oxygen (O) and carbon monoxide (CO), are adsorbed on a palladium (Pd) surface. The surface phase diagram of the system was studied in detail using DFT calculations.[8] The number of molecules to be adsorbed is determined using the two-dimensional parameters $\{N_{\mathrm{O}}, N_{\mathrm{CO}}\}$. Here, we consider the adsorption on the 2×2 and 4×4 surface structures of Pd. On the 2×2 surface, when four oxygen atoms are adsorbed, the top layer of the Pd slab is completely oxidized. Then, when $N_{\mathrm{O}} \geq 4$, $N_{\mathrm{O}} - 4$ oxygen atoms are absorbed on the top layer PdO surface. In preliminary calculations, we confirmed that the adsorption structures become unstable when more than five molecules are adsorbed on the surface. Therefore, except for oxidized oxygen, the maximum number of molecules adsorbed is four. This treatment is the same as that used in a previous study.[8] In this case, there are 29 conditions for $\{N_{\mathrm{O}}, N_{\mathrm{CO}}\}$ (see Table S1). On the other hand, in the case of the 4×4 surface, for $N_{\mathrm{O}} \geq 16$, the oxidized surface is considered, and a maximum of 16 molecules can be adsorbed except for oxidized oxygen. In addition, we consider the case in which the number of adsorbed molecules is even. Based on that, there are 89 possible conditions for $\{N_{\mathrm{O}}, N_{\mathrm{CO}}\}$ (see Table S2).

Under all these conditions, stable adsorption structures were searched using the constrained minima hopping method and Matlantis, and the adsorption energies $E_{\mathrm{abs}}(N_{\mathrm{O}}, N_{\mathrm{CO}})$ were calculated in advance. This enabled us to determine the optimal solution for the surface phase diagram. The adsorption energies are shown in Figs. 2(a) and 2(b). The stable structures are summarized in Tables S1 and S2. For the 2×2 surface, a stable adsorption structure could not be found for only one condition, i.e., $\{N_{\mathrm{O}}, N_{\mathrm{CO}}\} = \{4, 4\}$. Meanwhile, in the case of the 4×4 surface, no stable structure was found under 39 conditions. In general, adsorption energy tends to decrease as the number of adsorbed atoms increases. Therefore, N_{O} and N_{CO} can be better descriptors for predicting $E_{\mathrm{abs}}(N_{\mathrm{O}}, N_{\mathrm{CO}})$. To confirm this, we checked the prediction accuracy using the GPR model. The distributions of the test data using leave-one-out cross-validation are shown in Figs. 2(c) and 2(d). For the dataset, only the conditions where stable structures could be found were used. The R^2 value is high, and we confirmed that the adsorption energy can be predicted by the number of adsorbed adsorbates. The obtained result was consistent with an existing study that the adsorption energy strongly depends on the coverage of the adsorbed molecules.[29]

After completing the adsorption energy calculations for all structures, we plot a surface phase diagram. For -2.5 eV $\leq \Delta\mu_{\mathrm{O}} \leq 0$ eV and -2.5 eV $\leq \Delta\mu_{\mathrm{CO}} \leq 0$ eV, the surface phase diagrams are shown in Fig. 3. Note that these diagrams are not results of our proposed BBO method but results of adsorption energy calculations for all stable structures. Following the reported Pd–O–CO surface phase diagram,[8,9] the bulk PdO phase is also considered, as shown in Fig. 3. In comparison to the 2×2 surface, many more types of structures appeared in the 4×4 surface, and a substantial surface phase diagram is obtained by increasing the size of the surface. In addition, $\Delta\mu_{\mathrm{O}}$ and $\Delta\mu_{\mathrm{CO}}$ are discretized in increments of 0.05, and the sum of the adsorption free energies for the structures appearing at each point is defined as S_{opt} (shown in Fig. 3). Notably, the obtained phase diagram is slightly different from that of a previous study using DFT calculations,[8] which is attributed to the different conditions required for the number of molecules to be adsorbed and the different methods used for calculating the adsorption energy. The purpose of our study is not to plot an exact surface phase diagram but to verify the performance of BBO. The aim of the following demonstration is to obtain these phase diagrams shown in Fig. 3 with a smaller

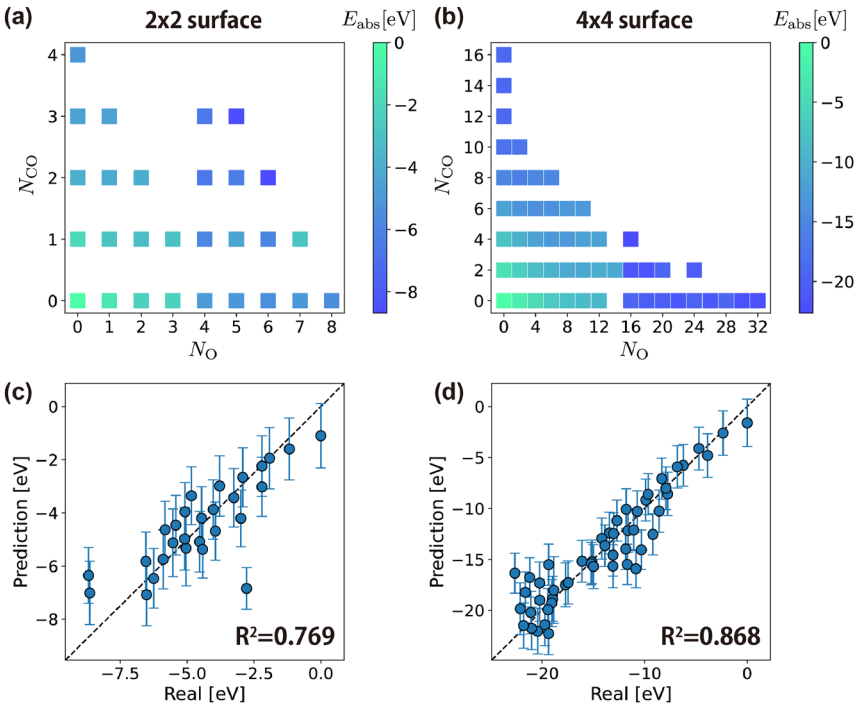

FIG. 2. Adsorption energy depending on the numbers of O atom N_O and CO molecule N_{CO} for (a) 2×2 and (b) 4×4 surfaces. When $N_O \geq 4$ for the 2×2 surface and $N_O \geq 16$ for the 4×4 surface, the top layer of Pd slab was treated as an oxidized surface, i.e., a PdO surface. The prediction results of adsorption energy from N_O and N_{CO} using the GPR model are shown for (c) 2×2 and (d) 4×4 surfaces. The mean and variance values of test data using leave-one-out cross validation are plotted.

number of calculations to explore the stable structures as much as possible.

Based on these results, the proposed BBO method is used to verify the performance. There are conditions for the number of adsorbates in which no stable structure could be found; however, these conditions are also included in the search space for verification. This is because the stability of the structure is known only after the simulation. If an unstable case is selected in the iterative calculation, the adsorption energy is regarded as 1, which is sufficiently high. Five different pairs of $\{N_O, N_{CO}\}$ are randomly selected as the initial data for the iterative calculations in BBO. For each BBO cycle, a surface phase diagram is obtained using only the conditions investigated at that time. When the number of investigated conditions is M, the sum of the adsorption free energies for the structures appearing at each point is defined as $S(M)$ on the discretized adsorption phase diagram in increments of 0.05. This value is larger

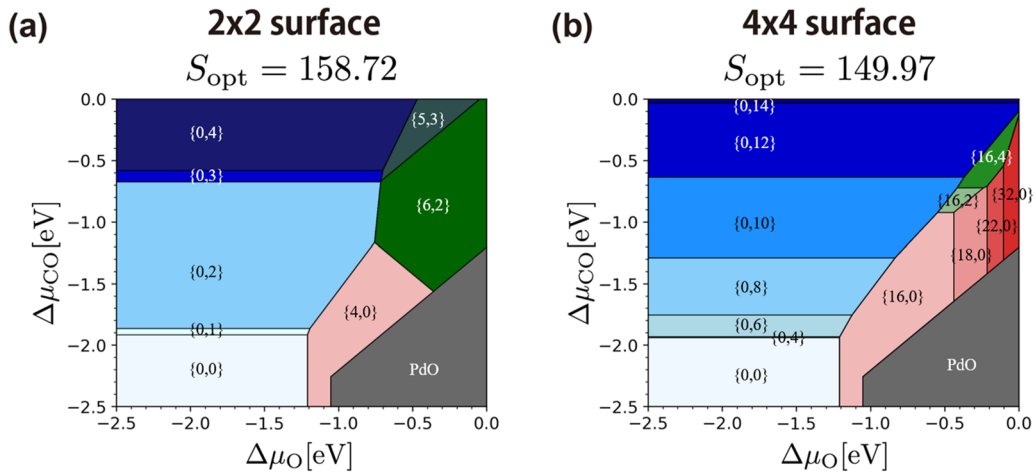

FIG. 3. Surface phase diagram depending on the chemical potentials $\Delta\mu_O$ and $\Delta\mu_{CO}$ for (a) 2×2 and (b) 4×4 surfaces. The $\{N_O, N_{CO}\}$ and S_{opt} values are also presented. These surface diagrams are plotted by all adsorption energies for all stable structures. The stable structures are summarized in Tables S1 and S2.

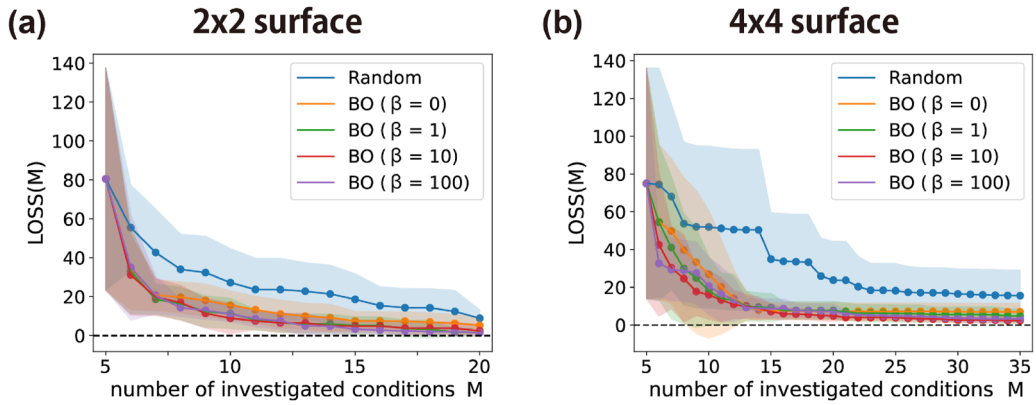

FIG. 4. Loss function LOSS(M) vs the number of investigated conditions M by the proposed BBO method for (a) 2 × 2 and (b) 4 × 4 surfaces. In each cycle of BBO, the number of investigated conditions is increased by one. The average of the results for ten independent runs with different initial data and the standard deviation are shown as lines and shaded areas, respectively.

than S_{opt} because the number of investigated conditions is small. Therefore, we define the loss function for the accuracy of the phase diagram as follows:

$$\mathrm{LOSS}(M) = S(M) - S_{\mathrm{opt}}. \tag{5}$$

The iteration dependence of LOSS(M) is shown in Fig. 4. Ten independent trials with different initial data are performed to calculate the statistical error for random initial selections, and the mean and variance of LOSS(M) are evaluated. In addition, the value of β in Eq. (2) is changed, and the optimization performance is compared with random selection, where the number of adsorbates is randomly selected in each cycle. The results show that the proposed BBO method provides a better LOSS(M) than random selection, and a detailed surface adsorption phase diagram can be obtained even if the number of investigated conditions is small. For the complex 4 × 4 surface, $\beta = 10$ is optimal, thus indicating that the search for the adsorption phase diagram can be accelerated by taking into account the variance of the prediction, like active learning. If our proposed method is adapted to any other surface phase diagram, the better β needs to be adjusted for each diagram calculation. On the other hand, our result shows that one strategy is to choose β such that the second term in Eq. (2) has sufficient influence. It is also possible to perform the search by changing the β in each step. The method for determining the proper β in any system is a topic we will study in the future.

IV. CONCLUSION

In conclusion, we proposed a BBO technique to investigate surface phase diagrams with the smallest possible number of calculations. With our technique, the surface phase diagrams of a palladium surface where oxygen and carbon monoxide were adsorbed were investigated. Two different surface sizes were considered, and a more complex result was obtained using a larger system. Therefore, adsorption on a larger surface should be considered in the calculations to approach the experimental systems. Overall, we believe that BBO can be used to treat wider surfaces by reducing the number of stable structure calculations. In this study, a neural network potential was used to rapidly calculate the adsorption energy. Furthermore, the constrained minima hopping method, which is a conventional method, was adopted to search for stable structures. Machine learning-assisted optimization methods will also be used for stable structure searches. By accelerating the entire method with machine learning, a surface phase diagram that can explain the details of the experiment will be rapidly provided.

SUPPLEMENTARY MATERIAL

Supplementary material Note A: Calculation methods of adsorption energy. Table S1: Stable structures of 2 × 2 surfaces with adsorbate and adsorption energy E_{abs}. Table S2: Stable structures of 4 × 4 surfaces with adsorbate and adsorption energy E_{abs}.

ACKNOWLEDGMENT

This study was performed under the MMC-NIMS Center of Excellence for Materials Informatics Research.

AUTHOR DECLARATIONS

Conflict of Interest

The authors have no conflicts to disclose.

Author Contributions

Makoto Urushihara: Conceptualization (equal); Investigation (equal); Software (equal); Supervision (equal); Validation (equal); Visualization (equal); Writing – review & editing (equal). **Kenji Yamaguchi**: Investigation (supporting); Writing – review & editing (equal). **Ryo Tamura**: Conceptualization (equal); Investigation (equal); Software (equal); Supervision (equal); Validation (equal); Visualization (equal); Writing – original draft (equal).

DATA AVAILABILITY

The data that support the findings of this study are available from the corresponding authors upon reasonable request.

REFERENCES

[1]Y. Kangawa, T. Akiyama, T. Ito, K. Shiraishi, and T. Nakayama, "Surface stability and growth kinetics of compound semiconductors: An ab initio-based approach," Materials **6**(8), 3309–3360 (2013).

[2]H. Li, Y. Jiao, K. Davey, and S.-Z. Qiao, "Data-driven machine learning for understanding surface structures of heterogeneous catalysts," Angew. Chem. **135**(9), e202216383 (2023).

[3]H. A. Hansen, J. Rossmeisl, and J. K. Nørskov, "Surface Pourbaix diagrams and oxygen reduction activity of Pt, Ag and Ni(111) surfaces studied by DFT," Phys. Chem. Chem. Phys. **10**(25), 3722–3730 (2008).

[4]M. Urushihara, K. Chan, C. Shi, and J. K. Nørskov, "Theoretical study of EMIM+ adsorption on silver electrode surfaces," J. Phys. Chem. C **119**(34), 20023–20029 (2015).

[5]D. Gustinčič and A. Kokalj, "A DFT study of adsorption of imidazole, triazole, and tetrazole on oxidized copper surfaces: Cu2O(111) and Cu2O(111)-w/o-CuCUS," Phys. Chem. Chem. Phys. **17**(43), 28602–28615 (2015).

[6]G. A. Ferguson, V. Vorotnikov, N. Wunder, J. Clark, K. Gruchalla, T. Bartholomew, D. J. Robichaud, and G. T. Beckham, "Ab initio surface phase diagrams for coadsorption of aromatics and hydrogen on the Pt(111) surface," J. Phys. Chem. C **120**(46), 26249–26258 (2016).

[7]L. Chen, J. W. Medlin, and H. Grönbeck, "On the reaction mechanism of direct H_2O_2 formation over Pd catalysts," ACS Catal. **11**(5), 2735–2745 (2021).

[8]J. Rogal, K. Reuter, and M. Scheffler, "First-Principles statistical mechanics study of the stability of a subnanometer thin surface oxide in reactive environments: CO oxidation at Pd(100)," Phys. Rev. Lett. **98**(4), 046101 (2007).

[9]J. Rogal, K. Reuter, and M. Scheffler, "CO oxidation at Pd(100): A first-principles constrained thermodynamics study," Phys. Rev. B **75**(20), 205433 (2007).

[10]K. Terayama, M. Sumita, R. Tamura, and K. Tsuda, "Black-box optimization for automated discovery," Acc. Chem. Res. **54**(6), 1334–1346 (2021).

[11]K. Terayama, R. Tamura, Y. Nose, H. Hiramatsu, H. Hosono, Y. Okuno, and K. Tsuda, "Efficient construction method for phase diagrams using uncertainty sampling," Phys. Rev. Mater. **3**(3), 033802 (2019).

[12]C. Dai and S. C. Glotzer, "Efficient phase diagram sampling by active learning," J. Phys. Chem. B **124**(7), 1275–1284 (2020).

[13]Y. Tian, R. Yuan, D. Xue, Y. Zhou, Y. Wang, X. Ding, J. Sun, and T. Lookman, "Determining multi-component phase diagrams with desired characteristics using active learning," Adv. Sci. **8**(1), 2003165 (2021).

[14]S. Ament, M. Amsler, D. R. Sutherland, M.-C. Chang, D. Guevarra, A. B. Connolly, J. M. Gregoire, M. O. Thompson, C. P. Gomes, and R. B. van Dover, "Autonomous materials synthesis via hierarchical active learning of nonequilibrium phase diagrams," Sci. Adv. **7**(51), eabg4930 (2021).

[15]K. Terayama, K. Han, R. Katsube, I. Ohnuma, T. Abe, Y. Nose, and R. Tamura, "Acceleration of phase diagram construction by machine learning incorporating Gibbs' phase rule," Scr. Mater. **208**, 114335 (2022).

[16]R. Tamura, G. Deffrennes, K. Han, T. Abe, H. Morito, Y. Nakamura, M. Naito, R. Katsube, Y. Nose, and K. Terayama, "Machine-learning-based phase diagram construction for high-throughput batch experiments," Sci. Technol. Adv. Mater.:Methods **2**(1), 153–161 (2022).

[17]Z. W. Ulissi, A. R. Singh, C. Tsai, and J. K. Nørskov, "Automated discovery and construction of surface phase diagrams using machine learning," J. Phys. Chem. Lett. **7**(19), 3931–3935 (2016).

[18]A. A. Peterson, "Global optimization of adsorbate–surface structures while preserving molecular identity," Top. Catal. **57**(1–4), 40–53 (2014).

[19]A. H. Larsen, J. J. Mortensen, J. Blomqvist, I. E. Castelli, R. Christensen, M. Dułak, J. Friis, M. N. Groves, B. Hammer, C. Hargus, E. D. Hermes, P. C. Jennings, P. B. Jensen, J. Kermode, J. R. Kitchin, E. L. Kolsbjerg, J. Kubal, K. Kaasbjerg, S. Lysgaard, J. B. Maronsson, T. Maxson, T. Olsen, L. Pastewka, A. Peterson, C. Rostgaard, J. Schiøtz, O. Schütt, M. Strange, K. S. Thygesen, T. Vegge, L. Vilhelmsen, M. Walter, Z. Zeng, and K. W. Jacobsen, "The atomic simulation environment—A Python library for working with atoms," J. Phys.: Condens. Matter **29**(27), 273002 (2017).

[20]S. Takamoto, C. Shinagawa, D. Motoki, K. Nakago, W. Li, I. Kurata, T. Watanabe, Y. Yayama, H. Iriguchi, Y. Asano, T. Onodera, T. Ishii, T. Kudo, H. Ono, R. Sawada, R. Ishitani, M. Ong, T. Yamaguchi, T. Kataoka, A. Hayashi, N. Charoenphakdee, and T. Ibuka, "Towards universal neural network potential for material discovery applicable to arbitrary combination of 45 elements," Nat. Commun. **13**(1), 2991 (2022).

[21]MATLANTIS, "Matlantis."

[22]H. Sampei, K. Saegusa, K. Chishima, T. Higo, S. Tanaka, Y. Yayama, M. Nakamura, K. Kimura, and Y. Sekine, "Quantum annealing boosts prediction of multimolecular adsorption on solid surfaces avoiding combinatorial explosion," JACS Au **3**(4), 991–996 (2023).

[23]T. M Dieb, Z. Hou, and K. Tsuda, "Structure prediction of boron-doped graphene by machine learning," J. Chem. Phys. **148**(24), 241716 (2018).

[24]M. Urushihara, M. Karube, K. Yamaguchi, and R. Tamura, "Optimization of core–shell nanoparticles using a combination of machine learning and ising machine," Adv. Photonics Res. **4**(12), 2300226 (2023).

[25]J. H. Montoya and K. A. Persson, "A high-throughput framework for determining adsorption energies on solid surfaces," npj Comput. Mater. **3**(1), 14 (2017).

[26]C. Martí, S. Blanck, R. Staub, S. Loehlé, C. Michel, and S. N. Steinmann, "DockOnSurf: A Python code for the high-throughput screening of flexible molecules adsorbed on surfaces," J. Chem. Inf. Model. **61**(7), 3386–3396 (2021).

[27]F. Pedregosa, G. Varoquaux, A. Gramfort, V. Michel, B. Thirion, O. Grisel, M. Blondel, P. Prettenhofer, R. Weiss, V. Dubourg, J. Vanderplas, A. Passos, D. Cournapeau, M. Brucher, M. Perrot, and É. Duchesnay, "Scikit-learn: Machine learning in Python," J. Mach. Learn. Res. **12**(85), 2825–2830 (2011).

[28]B. Shahriari, K. Swersky, Z. Wang, R. P. Adams, and N. de Freitas, "Taking the human out of the loop: A review of Bayesian optimization," Proc. IEEE **104**(1), 148–175 (2016).

[29]J. R. Kitchin, "Correlations in coverage-dependent atomic adsorption energies on Pd(111)," Phys. Rev. B **79**(20), 205412 (2009).